Double-difference tomography at Mt Etna volcano: Preliminary results

*Vadim Monteiller[1], Jean-Luc Got[1], D. Patanè[2], G. Barberi[2], O. Cocina[2]

[1] LGIT, Université de Savoie, CNRS, 73376 Le Bourget-du-Lac, France
[2] INGV, Sezione di Catania, 95125, Italy

* Corresponding author

Abstract

We performed a preliminary double-difference tomographic study using earthquake data recorded by the INGV-Catania seismic network during the large seismic and eruptive crisis of 2002-2003 at Mt Etna volcano. Compared to previous models, first results presented from the inversion of travel-time differences, tend to show an increase in the velocity contrast between the fast core and the slow periphery of the volcano.

Introduction – Framework and Method

Mt Etna volcano is an atypical volcano that has a complex geodynamic and magmatic history associated with the island of Sicily and the southern Apeninnes. It has erupted magmas of various compositions (from tholeiitic to trachytic) that have produced various deposits, from the early (0.5 Ma) pillow lavas of Acicastello to ignimbrites of Biancavilla (15 ka). Mt Etna has experienced numerous caldera collapses. For example the Valle del Bove, whose most recent collapse occurred 3,500 years ago, is interpreted as a major catastrophic sector collapse similar to that of Mount St Helens in May 1980. Smaller but more recent collapsing structures have also been identified. Drainage of large volumes of magma from possible storage areas also occurs (perhaps related to caldera collapse), for example in 1669 when the lava flows reached the town of Catania and the coastline. Understanding the volcano structure is therefore an important task to mitigate the volcanic and seismic hazard in this region. This may be carried out using seismic tomography.

Earthquake travel-time tomography has previously been used to develop a volcano velocity model for Mt Etna (e.g. Patanè et al., 2006; Patanè et al., 2003; Laigle et al., 2000). The question addressed herein is whether these results can be improved by using differential times. We therefore carried out a preliminary application of double-difference tomography to earthquake data recorded at Mt Etna by the INGV-Catania seismic network (50 stations in a 50 km x 50 km area) between October 2002 and January 2003. During this eruption 329 earthquakes were recorded and gave well-picked P- and S-wave arrival-times. Although the data set is limited, the very dense seismic network near Mt Etna summit provides the possibility of imaging the active volume within the structure. The first goal of this study is to investigate the spatial distribution of the resolution with this data set. A second aim is to search for similar earthquakes during the crisis, to compute a double-difference tomographic model with accurate cross-correlation time delays within a limited time period. This might be a way to improve the 4D tomographic result of Patanè et al. (2006). We also investigated the power of using picking differences in a double-difference algorithm, by using an adapted norm (the *sech* norm).

In this study we used the tomographic algorithm of Monteiller et al. (2005). Travel times are computed by solving the Eikonal equation using a finite-difference approach (Podvin and Lecomte, 1991) and *a posteriori* ray-tracing. It allows the computation of travel times with a relative accuracy better than 10^{-5}. The inverse problem is solved by using a probabilistic approach (Tarantola and Valette, 1982). It takes into account a realistic pdf (probability density function) to describe the error in travel times or time delays. As picking error distribution is better represented by a *sech* (hyperbolic secant) function than a gaussian function, we used a *sech* pdf in our tomographic inversion. The *sech* pdf behaves as a gaussian pdf for small errors, and as a L1-norm for large outliers. Such large outliers that characterize the picking difference distribution are therefore correctly taken into account during the inversion.

The probabilistic approach used allows an optimal regularization through the use of an *a priori* model covariance: standard deviation σ and correlation length λ. This is achieved by the computation of an accurate approximation of the inverse *a priori* covariance matrix, for the case of a L1-norm covariance kernel (Monteiller et al., 2005). This approximation is pre-computed, hence its application is extremely simple and fast. The L1-norm kernel exhibits very favourable characteristics for tomographic inversion as it keeps the stable, data-controlled, high-wavenumber fluctuations in the velocity model (Monteiller et al., 2005).

P- and S-wave travel-time tomography

A travel-time tomography was initially performed using P-wave arrival times. A volume of 140 km x 140 km horizontally x 25 km vertically, horizontally centered on the Mt Etna volcano summit was selected. This volume is sampled by 131,066 nodes with a 2-km horizontal interval and 1-km vertical interval. We used 4,183 P-wave and 980 S-wave arrival-times. The tomographic model of Patanè et al. (2006) was used as an initial model and initial positions were taken from the earthquake catalog compiled by the INGV-CT observatory. After exploring a wide range of velocity variances and correlation lengths, we choose results corresponding to the optimal quantity of *a priori* information (σ_V = 750m/s and λ = 2.5 km). Minimum RMS reached is 0.18 s.

Results show that P- and S-wave travel-time tomographic inversions are correctly resolved in a major part of the considered volume. Checkerboard tests (Figure 1a) were performed on the final velocity model. Travel times were computed using a 1% sinusoidal velocity perturbation (wavelength: 10 km horizontally, 2 km vertically) of the final P-wave velocity model. These tests show that the density of seismic stations around the summit of Mt Etna allows the medium to be well resolved in this region. The results illustrate that the horizontal resolution in the summit region is less than 5 km, at a depth of 1 to 4 km. The medium in the summit region can be reconstructed correctly from 329 events only; using more events can improve the resolution. P-wave velocity maps (Figure 1b) show two concentric features in the summit region: a fast central cylindrical core, probably of intrusive origin, surrounded by a slower body.

Double-difference tomography

In this preliminary work, travel-time differences from the 329 earthquakes were used to relocate the events and re-compute the velocity parameters. Earthquake pairs were selected such that their travel-time differences were larger than their estimated 0.075s uncertainty, and smaller than 1s in order to avoid processing large quantities of non-significant data.

The probabilistic algorithm of Monteiller et al. (2005) was employed to compute the velocity parameters using these differential data (*sech* norm was used). The optimal quantity of *a priori* information was experimentally determined (again σ_V = 750m/s and λ = 2.5 km) and used to adequately regularize the solution. Minimum RMS reached is 0.10 s.

Checkerboard tests indicate that the model may be correctly reconstructed using earthquake pairs. Double-difference locations of the earthquakes occurring during the crisis show that a significant number of them occur along an elongated swarm, exhibiting a clear SW-NE trend along the North-East rift.

Our results show that the recovered P-wave travel-time tomographic model (Figure 2b) matches that shown in Figure 1b, particularly for greater depths. Differences between the two models (Figures 1b and 2b) in the well-resolved volumes are moderate and tend to increase the contrasts (5-10% faster in the center, 5% slower in the periphery). Notice that there is some competition between the 40% larger standard deviation (std) in travel-time difference (as compared to the std of travel-times) and the spatially restricted Fréchet kernel. The Vp/Vs model is quite similar to the one identified by Patanè et al. (2006) in the summit region. The South-West caldera exhibits low Vp/Vs ratios, especially at the edge of the caldera near the South rift between 1 and 3 km depth. Other zones exhibit high Vp/Vs ratios, especially in the South-West caldera below the collapsed section of the Valle del Bove. Further work will investigate these features in more detail.

Increasing the accuracy of these velocity models would however require further, more accurate, data. For that reason we have searched for similar earthquakes in our dataset. We first computed the generalized coherency matrix of the 329-event dataset and, based on a similarity criterion, we define 'equivalence classes'; an event belongs to a given equivalence class if it is more than 90% coherent (5-frequency sample smoothing) with at least one of the events of the class. In the same manner, we also compute the generalized cross-correlation matrix. In both cases we found 6 events that correlate well (coherency C > 0.9), and about 100 events with poorer coherency or cross-correlation coefficient (C ~ 0.8; CC ~ 0.7). The 6 well-correlated events can be accurately relocated (RMS residual ~ 7 milliseconds) along a SW-NE direction, whereas the 100 event set is relocated with a RMS residual of ~25 milliseconds. The results show that the larger event set is an ellipsoid, whose dimensions are related to the location uncertainty. Interestingly, despite the events being relatively close (200-500 m, as determined by their arrival-time difference location) they do not appear to be very similar, even after careful inspection of their waveform. This is similar to results reported by Barberi et al. (2004). It may be related to the fact that these events occurred during an eruption, i.e. they are associated with the fracturing of the rocks in traction rather than with the slip along a well-defined existing fault plane (as it occurs for the Kilauea volcano decollement plane or the creeping segment of the San Andreas fault). In the case of Mt Etna, no fault plane exists before the rupture, and the rupture planes at a small scale may have relatively heterogeneous geometric characteristics. A careful examination of the seismic traces show that these events often have a high-frequency onset followed by a long-period wavetrain (i.e. they are LP events), occurring very close to the advancing magma. In any case, there is insufficient information (cross-spectral or cross-correlation time delays) to improve the velocity model in a double-difference tomographic process. Future work will therefore concentrate on very similar events extracted within a larger database to improve this tomographic image. However, our results show that it will be difficult to simultaneously improve the time and spatial resolutions.

Conclusion

Although we have presented only initial results, some structural elements can be clearly identified. Double-difference location shows that earthquakes mainly occur along a SW-NE direction. Double-difference tomography results are quite similar to the travel-time tomography, enhancing slightly (5-10%) the velocity contrasts. The fast core may be interpreted as a solidified intrusive body. This high Vp intrusion, previously identified by other authors (see e.g. Chiarabba et al., 2004), is the main structural feature of the volcano. It confirms its intense history and reveals the accumulation of a large volume of non-erupted volcanic material feeding previous eruptive centres.

The low velocity structure at different depths surrounding the high velocity body can be related to:

- the presence of sedimentary terrains underlying the volcanic edifice and/or of zones of weakness with brittle behaviour and high degree of rock fracturing,
- areas that contain fluids migrating from the intrusion zone into fractured regions.

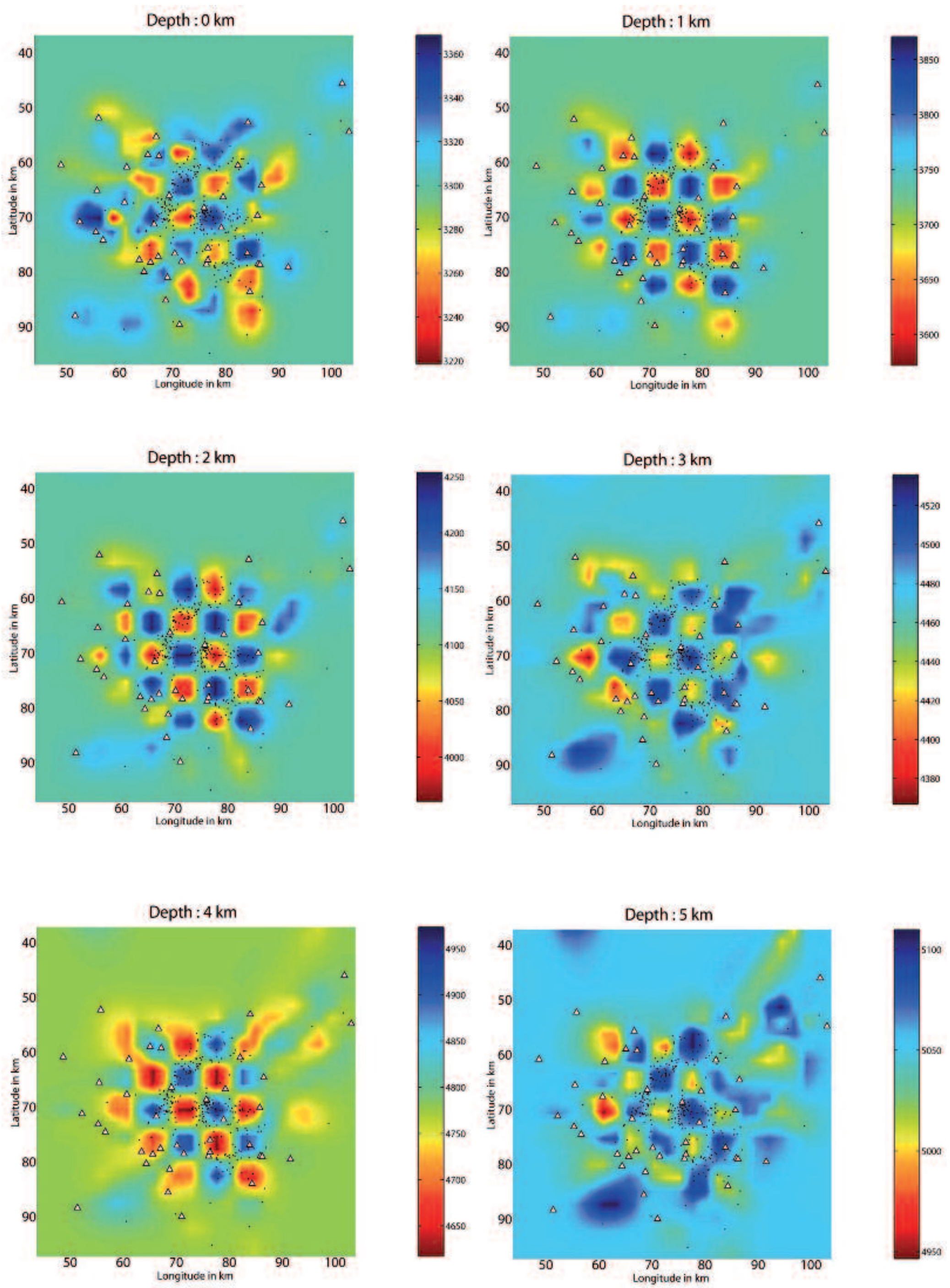

Figure 1. (a) Result of the checkerboard test performed with the earthquake-station geometry and the final tomographic model (see text for details). Triangles represent station locations. Colour scale indicates P-wave velocity in m/s.

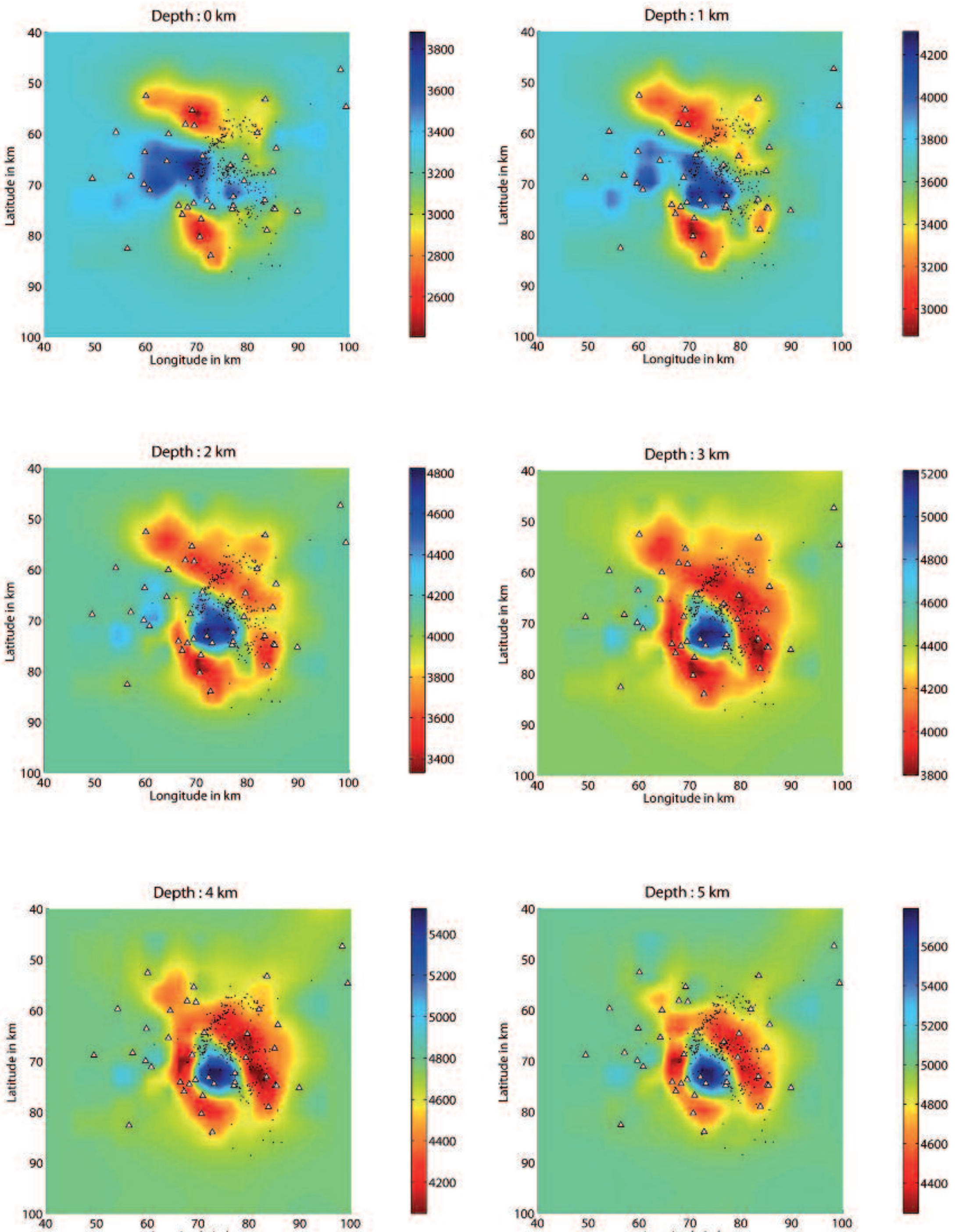

Figure 1. (b) Result of the tomographic inversion of P-wave travel-times, for the optimal *a priori* information. Triangles represent station locations. Colour scale indicates P-wave velocity in m/s.

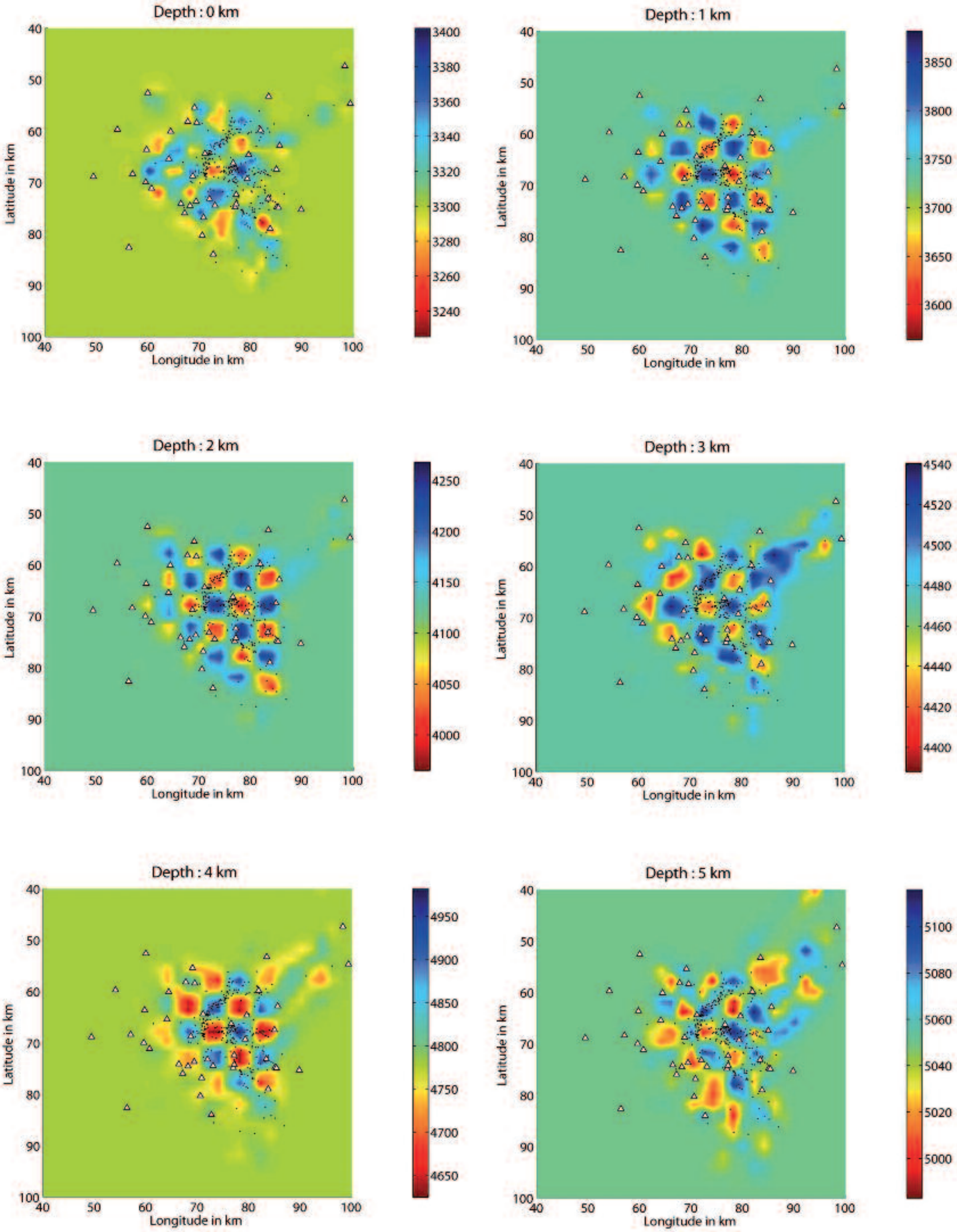

Figure 2. (a) Result of the checkerboard test performed with the earthquake-station geometry and the final double-difference tomographic model. Triangles represent station locations. Colour scale indicates P-wave velocity in m/s.

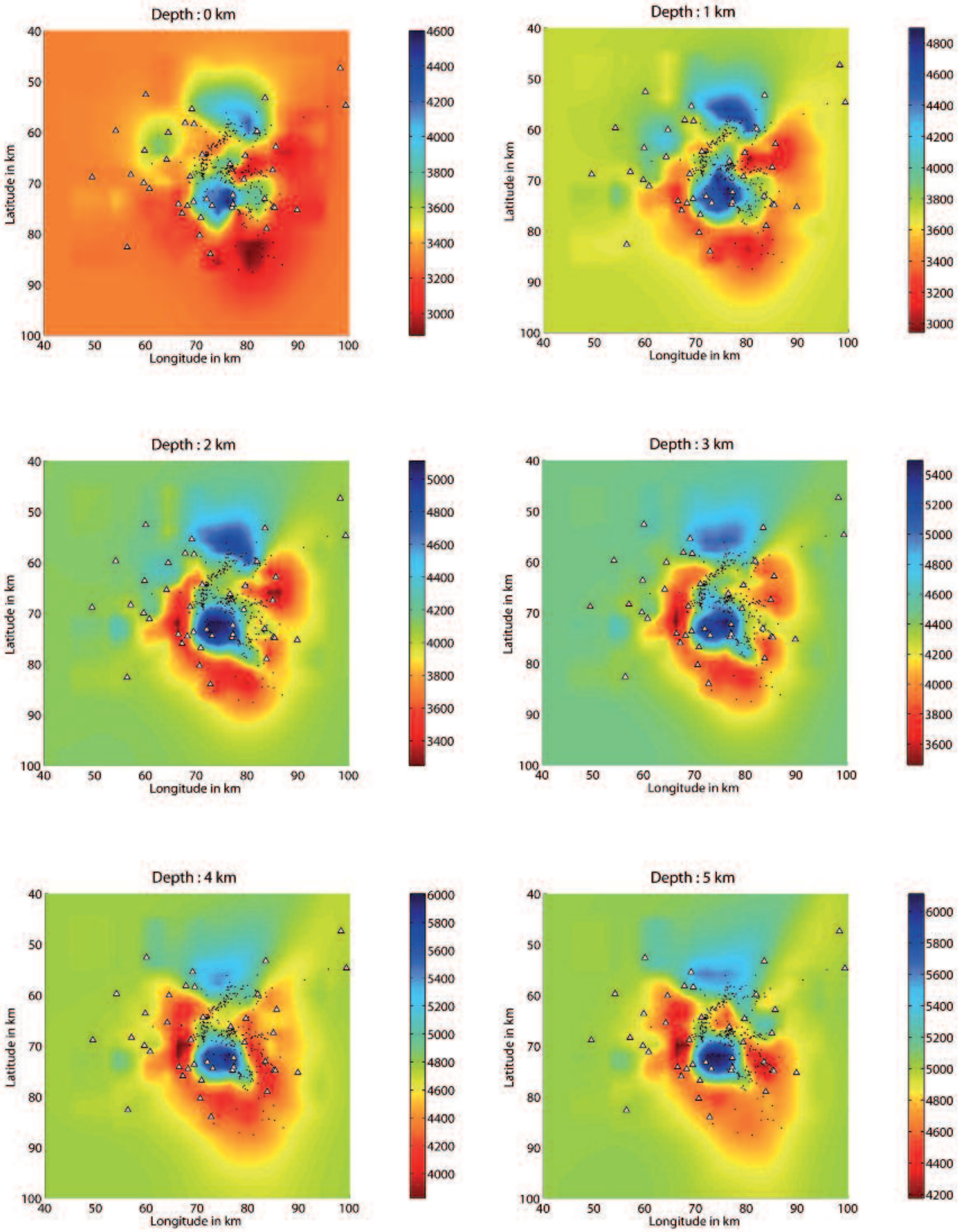

Figure 2. (b) Result of the double-difference P-wave tomographic inversion, using travel-time differences and the optimal *a priori* information. Triangles represent station locations. Colour scale indicates P-wave velocity in m/s.

References

Barberi, G., Cocina, O., Maiolino, V., Musumeci, C., Privitera, E., 2004. Insight into Mt Etna (Italy) kinematics during the 2002_2003 eruption as inferred from seismic stress and strain tensors. Geophys. Res. Lett. 31, doi:10.1029/2004GL020918.

Chiarabba, C., De Gori, P., Paranè, D., 2004. The Mt Etna plumbing system : the contribution of seismic tomography. In « Etna Volcano Laboratory », Bonnacorso A., Calvari, S., Coltelli, M., Del Negro C., Falsaperla, S. (Eds), AGY Geophysical Monograph Series, 91-110.

Laigle, M., Hirn, A., Sapin, M., Lépine, J.-C., Diaz, J., Gallart, J., Nicolich, R., 2000. Mount Etna dense array local earthquake P and S tomography and implications for volcanic plumbing. J. Geophys. Res. 105, 21633-21646.

Monteiller, V., Got, J.-L., Virieux, J., Okubo, P.G., 2005. An efficient algorithm for double-difference tomography and location in heterogeneous media, with an application to the Kilauea volcano. J. Geophys. Res., 110, B12306, doi:10.1029/2004JB003466.

Patanè, D., Chiarabba, C., De Gori, P., Bonaccorso, A., 2003. Magma ascent and the pressurization of Mt Etna's volcanic system. Science 299, 2061-2063.

Patanè, D., Barberi, G., Cocina, O., De Gori, P., Chiarabba, C., 2006. Time-resolved seismic tomography detects magma intrusions at Mount Etna. Science 313, 821-823.

Podvin, P., Lecomte I., 1991. Finite difference computation of traveltimes in very contrasted velocity models : a massively parallel approach and its associated tools. Geophys. J. Int., 105, 271-295.

Tarantola, A., Valette, B., 1982. Generalized nonlinear inverse problems solved using the least-squares criterion. Rev. Geophys. Space Phys., 20,